Supplement of Atmos. Chem. Phys., 14, 4779–4791, 2014
http://www.atmos-chem-phys.net/acp-14-4779-2014/
doi:10.5194/acp-14-4779-2014-supplement

Atmospheric Chemistry and Physics
Open Access

Supplement of

Sulfur hexafluoride (SF_6) emissions in East Asia determined by inverse modeling

X. Fang et al.

Correspondence to: X. Fang (fangxuekun@gmail.com)

Table S1 Summary of specific a priori emissions (Mg/yr) for China mainland, Taiwan region, South Korea, Japan and the entire Globe used in the reference inversion.

	Mainland China	Taiwan region	South Korea	Japan	Globe
2006	1299	125	669	205	6395
2007	1587	125	707	184	6965
2008	1695	119	728	159	7290
2009	1848	123	778	77	7657
2010	2091	123	692	78	8034
2011	2234	123	628	105	8412
2012	2470	123	628	105	8789

Table S2. Inversion performance for UC_adjust, UC and EDGAR inversions in 2008. The meanings of all statistical items are described in Table 2 in main text.

		B_a	B_b	E_a	E_b	$1 - E_b\ E_a$	r_a^2	r_b^2	r_{ea}^2	r_{eb}^2
Gosan	UC_adjust	0.165	0.044	0.73	0.61	16%	0.26	0.45	0.26	0.41
	UC	0.413	0.098	0.88	0.66	25%	0.10	0.37	0.09	0.35
	EDGAR	0.342	0.084	0.83	0.65	23%	0.15	0.40	0.00	0.39
Hateruma	UC_adjust	0.116	0.032	0.30	0.25	17%	0.47	0.58	0.36	0.48
	UC	0.183	0.043	0.36	0.25	32%	0.34	0.59	0.29	0.51
	EDGAR	0.149	0.046	0.30	0.25	16%	0.55	0.59	0.48	0.50
Cape Ochi-ishi	UC_adjust	0.068	0.003	0.16	0.12	26%	0.64	0.76	0.59	0.70
	UC	0.104	0.006	0.21	0.12	42%	0.41	0.74	0.56	0.69
	EDGAR	0.089	0.007	0.19	0.12	35%	0.55	0.75	0.61	0.69

Table S3. National a priori and a posteriori emissions (Mg/yr) from UC_adjust, UC and EDGAR inversions in 2008.

	UC_adjust		UC		EDGAR	
	A priori	A post	A priori	A post	A priori	A post
Mongolia	2	3	3	3	0	0
China	1702	2312	1473	2258	1876	2668
Taiwan region	119	261	26	183	179	268
North Korea	20	65	26	104	16	50
South Korea	728	624	55	450	227	541
Japan	159	302	159	328	183	292
East Asia	2730	3567	1742	3326	2481	3819

Table S4. Inversion performance from inversions using ECMWF, CFSR and FNL meteorological data for three stations in 2008. The symbols used are described in Table 2 in the main text.

		B_a	B_b	E_a	E_b	$1 - E_b\ E_a$	r_a^2	r_b^2	r_{ea}^2	r_{eb}^2
Gosan	ECMWF	0.165	0.044	0.73	0.61	16%	0.26	0.45	0.26	0.41
	Nest_ECMWF	0.184	0.031	0.70	0.59	16%	0.32	0.49	0.33	0.46
	CFSR	0.143	0.040	0.74	0.62	17%	0.23	0.43	0.24	0.38
	FNL	0.190	0.057	0.75	0.67	11%	0.23	0.35	0.24	0.31
Hateruma	ECMWF	0.116	0.032	0.30	0.25	17%	0.47	0.58	0.36	0.48
	Nest_ECMWF	0.122	0.029	0.31	0.23	26%	0.45	0.65	0.35	0.57
	CFSR	0.139	0.060	0.33	0.28	14%	0.40	0.49	0.28	0.37
	FNL	0.117	0.038	0.30	0.24	19%	0.49	0.62	0.40	0.53
Cape Ochi-ishi	ECMWF	0.068	0.003	0.16	0.12	26%	0.64	0.76	0.59	0.70
	Nest_ECMWF	0.069	0.005	0.16	0.12	27%	0.65	0.77	0.60	0.71
	CFSR	0.057	0.011	0.17	0.14	14%	0.57	0.64	0.49	0.55
	FNL	0.065	0.011	0.17	0.15	15%	0.56	0.63	0.48	0.54

Table S5. National a posteriori emissions (Mg/yr) from inversions using ECMWF, Nest_ECMWF, CFSR or FNL meteorological data in 2008.

	ECMWF	Nest_ECMWF	CFSR	FNL
Mongolia	3	5	20	19
China	2312	2355	2132	2204
Taiwan region	261	312	138	149
North Korea	65	100	37	124
South Korea	624	648	582	521
Japan	302	252	246	229
East Asia	3567	3672	3155	3246

Table S6. Inversion performance at Gosan, Hateruma and Cape Ochi-ishi for the 2006–2012 period. Mean and sd are the average observed mixing ratios and the corresponding standard deviation, respectively. N denotes the number of 3-hourly averaged observations. B_a and B_b denote the mean bias between the a priori concentrations and observations, and a posteriori concentrations and observations, respectively. E_a and E_b are the a priori and, a posteriori RMS errors for the full data set, respectively, including outliers. $1-E_b$ E_a represents the relative error reduction. E_b^n is the a posteriori error normalized with the standard deviation of the observed concentrations. r_a^2 and r_b^2 denote the squared Pearson correlation coefficients between the observations and the a priori and, respectively, a posteriori model results. r_{ba}^2 and $r_{bb}^2$are the squared Pearson correlation coefficients between the observations and the a priori baseline and, respectively, a posteriori baseline. r_{ea}^2 and r_{eb}^2 are the squared Pearson correlation coefficients between the observations and the a priori and a posteriori model concentrations, respectively, all with the a priori or a posteriori baseline subtracted.

Year	Station	Mean ppt	sd ppt	N	B_a ppt	B_b ppt	E_a ppt	E_b ppt	$1 - E_b\ E_a$ %	E_b^n %	r_a^2	r_b^2	r_{ea}^2	r_{eb}^2	r_{ba}^2	r_{bb}^2
2006	Hateruma	5.94	0.48	2146	0.081	0.045	0.43	0.42	2	87	0.24	0.26	0.13	0.14	0.14	0.14
	Cape Ochi-ishi	5.93	0.11	649	0.036	0.003	0.09	0.07	23	63	0.46	0.61	0.47	0.62	0.00	0.00
2007	Hateruma	6.41	0.34	2640	0.106	0.035	0.29	0.23	20	69	0.38	0.54	0.29	0.47	0.15	0.15
	Cape Ochi-ishi	6.10	0.16	2061	0.036	0.005	0.14	0.12	15	74	0.35	0.45	0.26	0.35	0.16	0.17
2008	Gosan	7.12	0.82	1655	0.165	0.044	0.73	0.61	16	75	0.26	0.45	0.26	0.41	0.00	0.08
	Hateruma	6.73	0.38	2611	0.116	0.032	0.30	0.25	17	66	0.47	0.58	0.36	0.48	0.16	0.18
	Cape Ochi-ishi	6.47	0.24	1829	0.068	0.003	0.16	0.12	26	50	0.64	0.76	0.59	0.70	0.23	0.26
2009	Gosan	7.45	1.17	1762	0.177	0.069	1.10	1.03	6	88	0.15	0.24	0.14	0.20	0.04	0.06
	Hateruma	7.09	0.39	2615	0.138	0.039	0.29	0.23	22	59	0.55	0.66	0.43	0.54	0.23	0.26
	Cape Ochi-ishi	6.75	0.18	2159	0.064	0.004	0.15	0.12	18	68	0.46	0.55	0.35	0.47	0.18	0.17
2010	Gosan	7.74	0.95	1938	0.220	0.058	0.72	0.62	14	66	0.49	0.58	0.48	0.57	0.01	0.04
	Hateruma	7.31	0.45	2588	0.169	0.060	0.40	0.33	18	72	0.39	0.50	0.35	0.44	0.07	0.12
	Cape Ochi-ishi	7.02	0.18	2464	0.062	0.001	0.16	0.14	11	78	0.38	0.43	0.27	0.32	0.19	0.20
2011	Gosan	8.06	1.27	1614	0.296	0.153	1.08	0.95	12	75	0.34	0.47	0.31	0.43	0.06	0.09
	Hateruma	7.58	0.32	2732	0.126	0.033	0.26	0.20	23	63	0.51	0.61	0.45	0.56	0.12	0.14
	Cape Ochi-ishi	7.45	0.26	2436	0.080	0.003	0.17	0.14	17	52	0.70	0.73	0.40	0.47	0.50	0.50
2012	Gosan	8.37	0.87	1742	0.222	0.040	0.72	0.64	10	74	0.39	0.45	0.38	0.45	0.01	0.01
	Hateruma	7.88	0.41	1989	0.137	0.032	0.33	0.25	24	60	0.49	0.65	0.36	0.54	0.24	0.24
	Cape Ochi-ishi	7.86	0.19	2379	0.082	0.010	0.16	0.13	15	70	0.51	0.52	0.34	0.36	0.25	0.25

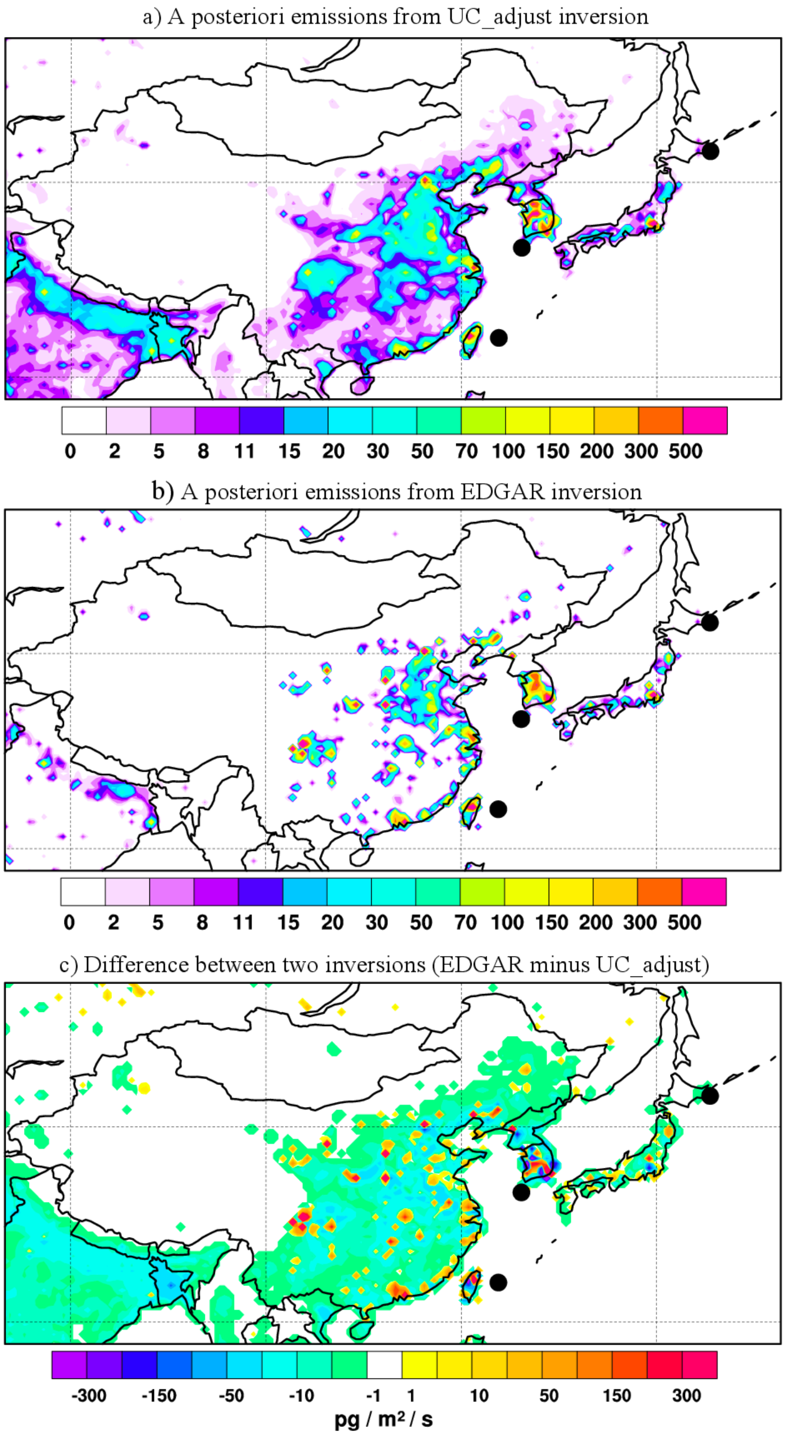

Figure S1. Maps of the a posteriori emissions from UC_adjust inversion (a), EDGAR inversion (b), and difference between two inversions (EDGAR minus UC_adjust; c) for 2008. Black dots denote the measurement stations.

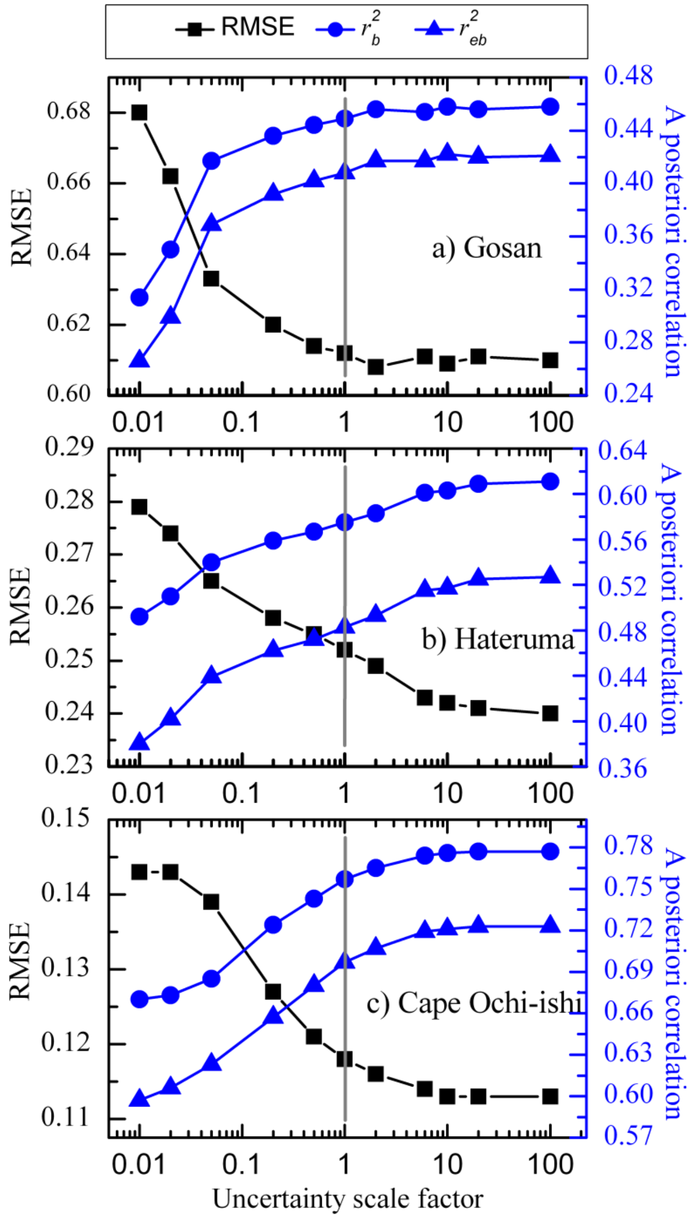

42

43 Figure S2. Dependence of a posteriori RMSE and squared correlation coefficients (r_b^2, r_{eb}^2) on the a priori emission uncertainty scale factor p for Gosan (a), Hateruma (b) and Cape Ochi-shi (c).

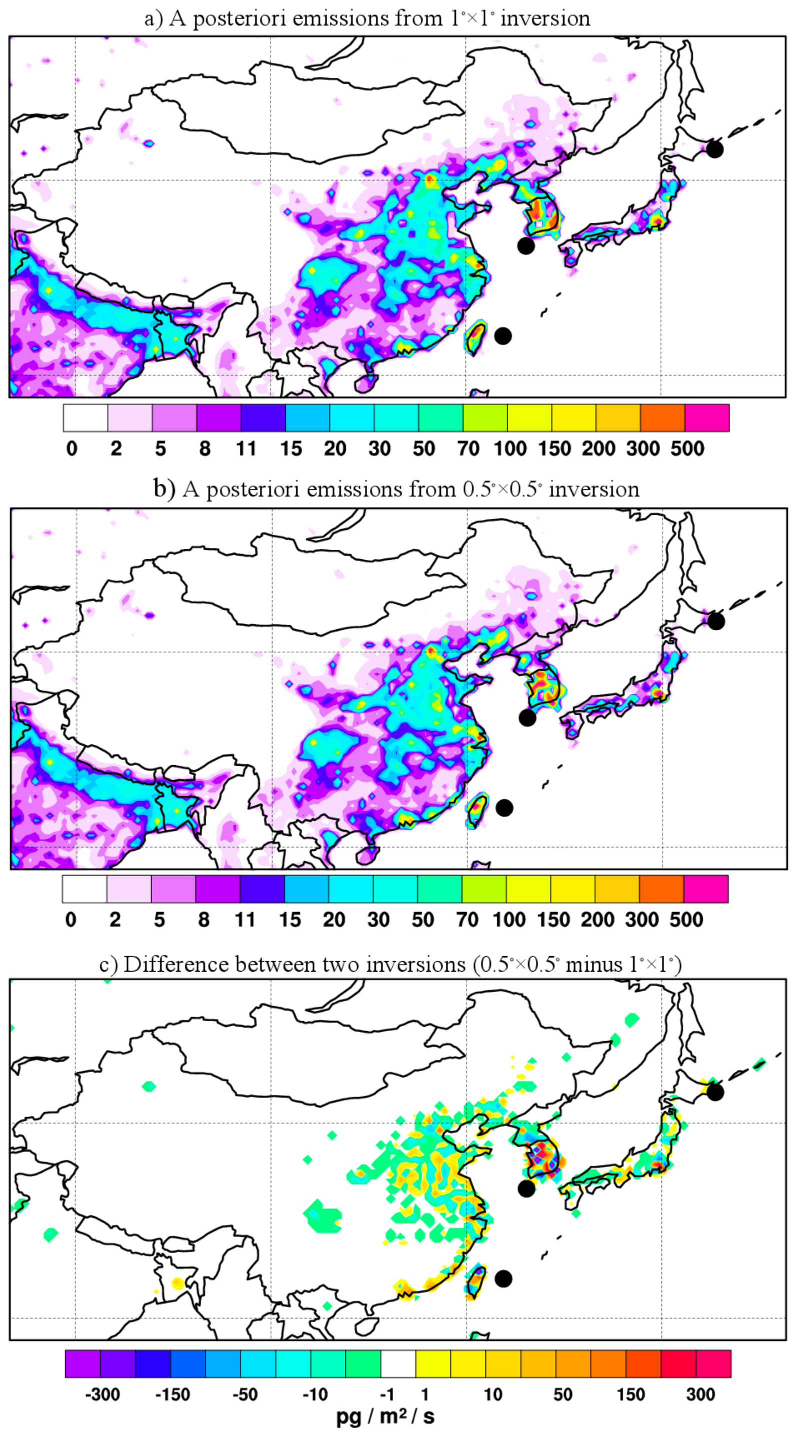

Figure S3. Maps of a posteriori emissions from inversions using 0.5°×0.5° grid cells (a), 1°×1° grid cells (b) and difference between these two inversions (c) for the year 2008. Black dots denote the measurement stations.

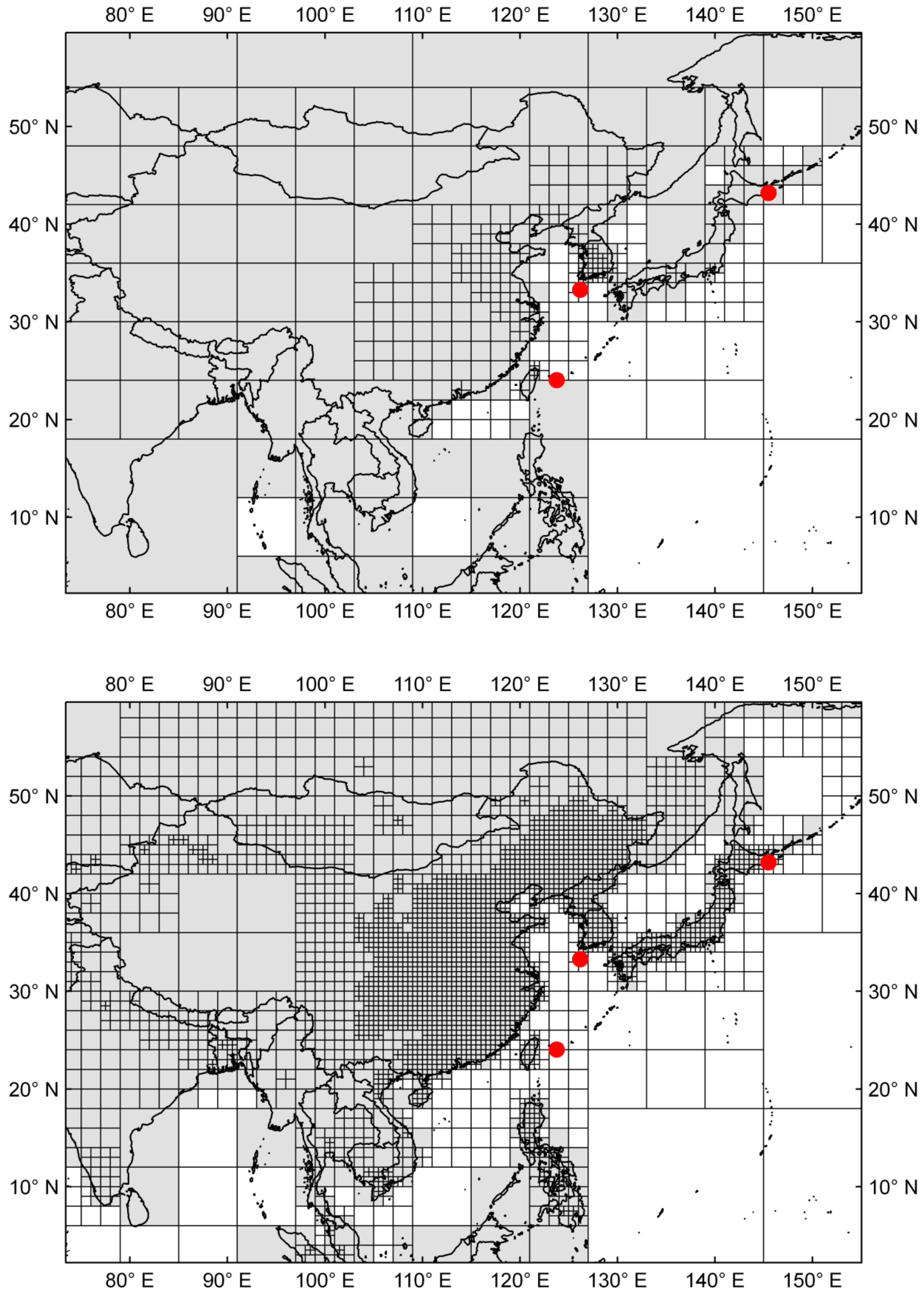

Figure S4. Maps of 546 (top panel) and 5323 (bottom panel) variable-resolution grid cells with highest resolution of 0.5°× 0.5° used in the inversion. The red dots denote the measurement stations. Gray boxes are considered in the inversion process and white boxes are not.

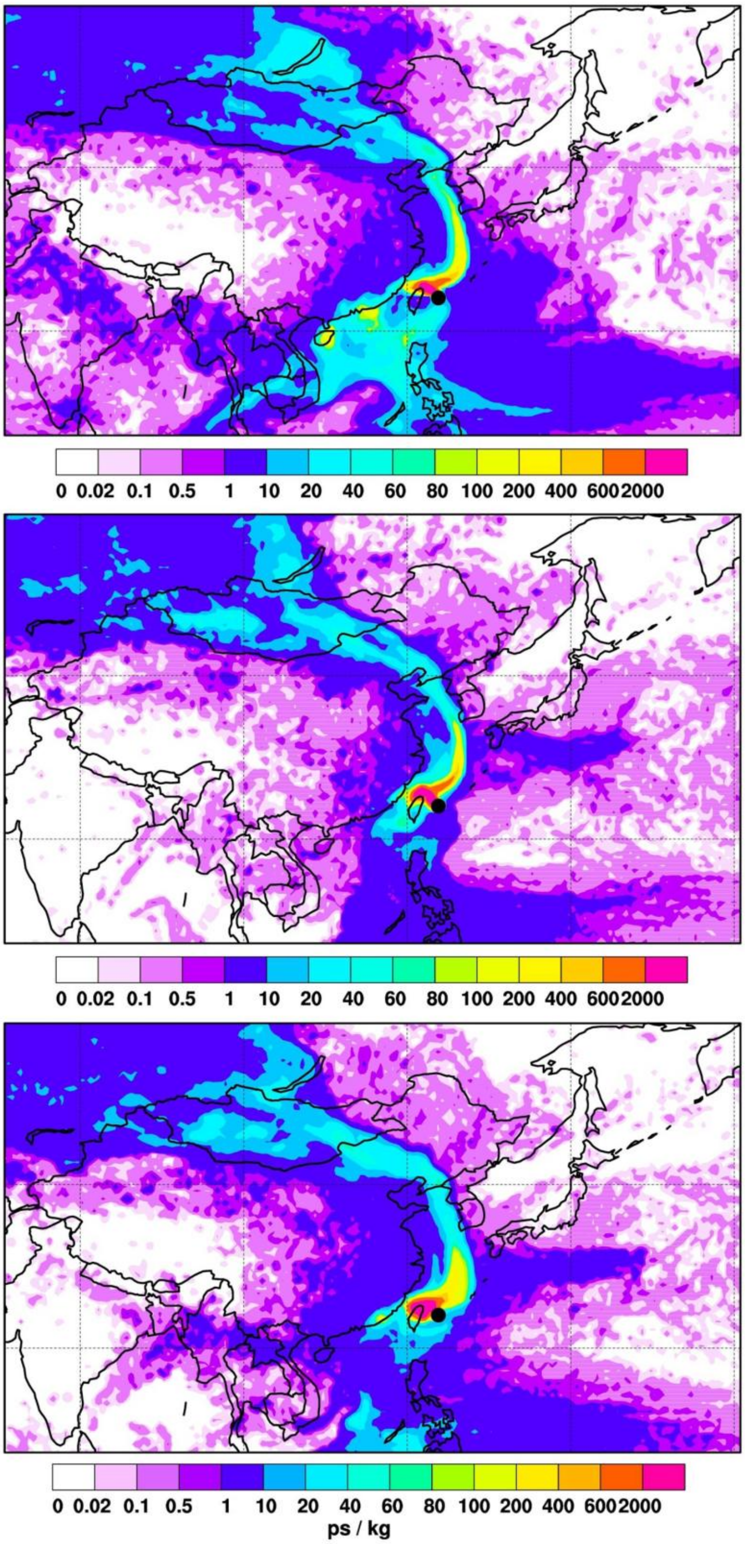

Figure S5. Emission sensitivity at 15:00 UTC on 8 May 2008 from simulation using ECMWF (top panel), CFSR (middle panel) and FNL (bottom panel) meteorological data at the Hateruma station.

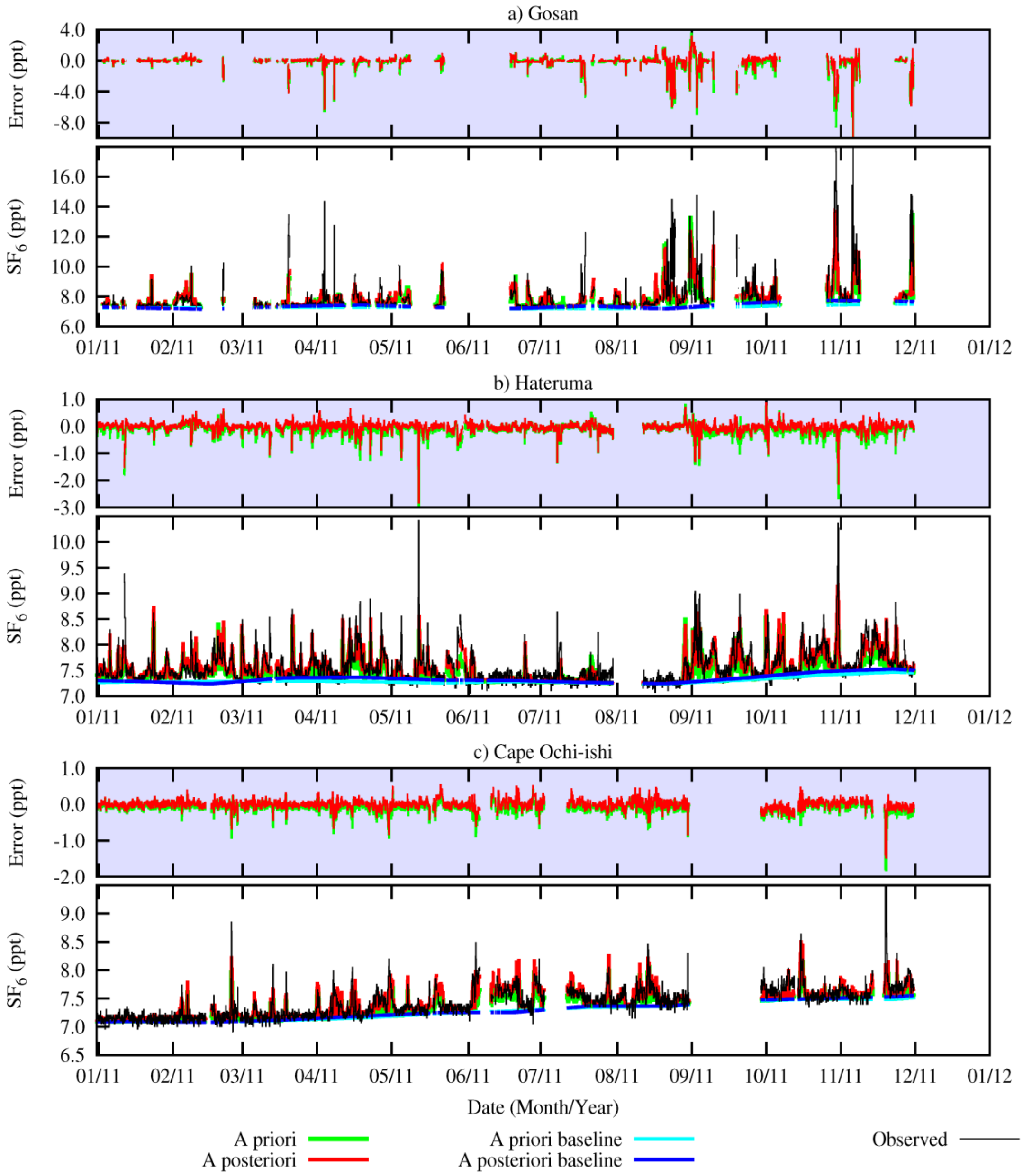

Figure S6. SF_6 time series for (a) Gosan, (b) Hateruma, and (c) Cape Ochi-ishi for the year 2011. For every station, the lower panels show the observed and modeled mixing ratios. Modeled mixing ratios are shown when using a priori (green line) and a posteriori emissions (red line). Corresponding a priori (cyan line) and a posteriori (blue line) baselines are also shown. The upper panels show the model errors when using the a priori emissions (green lines) and the a posteriori emissions (red lines).